Kinetic analysis of computer experiments on electron hydration dynamics

E. Keszei and S. Nagy
Eötvös University, H-1518 Budapest 112, P.O.B. 32, Hungary

T. H. Murphrey and P. J. Rossky
The University of Texas at Austin, Austin, Texas 78712-1167

(Received 30 March 1993; accepted 16 April 1993)

Based on a careful analysis of recent nonadiabatic dynamical simulations, a new mechanism is proposed to describe the hydration of electrons in pure water, and the solution of the corresponding set of differential equations is given. According to this mechanism, a thermalization via spontaneous de-excitations across a manifold of delocalized excited states is followed by a branching between a two-step hydration and a direct trapping path leading to the ground state of the hydrated electron. From a kinetic perspective, the most important results of the analysis derive from the temporal evolution of the electronic states in two different sets of simulation trajectories; one in which the electron initially possesses about 2 eV excess energy in the unrelaxed solvent, and another at an initial excess energy higher about 0.5 eV. Estimated characteristic rates for energy loss during thermalization are found to be identical for the two cases. However, branching ratios and characteristic times for the solvation steps show considerable differences, depending on the initial energy of the hot electrons injected into the water.

I. INTRODUCTION

After the first evidence[1] of two-photon ionization of pure water by ultraviolet laser pulses, and a thorough analysis of the energy dependence of the quantum yield and the products of the reaction[2] had been published, this technique became the exclusive experimental tool to study electron hydration dynamics in pure water.[3–8] As this reaction is practically complete within 1–1.5 ps, detailed kinetic information on this reaction necessitates a temporal resolution of about 100 fs. However, the resolution of the detection is not directly related to the width of the incident pump pulse, as the temporal evolution of the absorbance is convoluted with both the pump and the probe pulses *plus* the delay due to the refractive index difference between the two wavelengths.[3] As a result, the *effective pulse width*—which determines the instrumental resolution of the detection—is typically about three times greater than that of the pulse width of the laser light source. The convolution of the kinetic response with this effective pulse imposes severe limitations on the inference of detailed kinetic information from current pump and probe laser measurements.

Recent pump and probe measurements[3–8] revealed evidence that there are distinct precursor species of the fully relaxed hydrated electron. In the papers reporting these results, a simple two-step mechanism has been adopted, and has been found sufficient to explain all the ultrafast kinetic traces. The only modification to this mechanism has been proposed by Gauduel *et al.*, who suggested a similar two-step formation of an encounter pair in concentrated aqueous solutions, parallel to the hydrated electron formation.[5]

Prompted by the experimental results on the kinetics of electron hydration, molecular dynamics simulations also explored this reaction in suitable model systems.[9–14] The first study of electron trapping in pure water only explored the existence of "trapping sites," probing the sites with a "test charge" to evaluate the capacity of the traps to host an electron.[9] The first test of a scenario for the dynamical relaxation of an electron to its equilibrium state in a water bath was reported by Rossky and Schnitker,[10] but they were only able to simulate *electronically adiabatic* relaxation of the ground state in a water bath. The results did not match experimental observations, implying that other electronic states were important and leading to the original hypothesis that a well defined solvated excited state was involved. The advent of new molecular dynamics methods involving *nonadiabatic* transitions[11–13] enable the simulation of electronic relaxation with realistic model systems, and results obtained with them are generally consistent with experimental observations.[13,14]

Another refinement of the simulations is the use of *flexible water molecules*,[15–17] thus including intramolecular modes in the dynamical processes. All these elements have been put together in a recent simulation by Murphrey and Rossky.[14] Their results are in good agreement with recent experimental inferences on electron hydration kinetics, and, further, include complete, but as yet untapped information from a kinetic point of view.

The quality of the simulation data makes it possible to consider these simulations as computer experiments, and analyze them to suggest or probe the validity of alternative mechanistical models of the hydration process. There is no convolution in the simulated data, i.e., the instantaneous concentration, as a function of time, can directly be analyzed. This paper describes a thorough and careful kinetic analysis of the simulation results. In particular, we make the hypothesis here that these computer experiments describe the true physical processes occurring in the relaxation of excess electrons in water. We then use the detailed data to develop a corresponding kinetic model which we can assure captures the physical processes observed, and

 0021-9606/93/99(3)/2004/8/$6.00

the solutions to the corresponding equations are derived. The simulated data is then used to determine the relevant kinetic parameters that would be observed in an ideal experiment on this system if the data were analyzed on the basis of this model.

The paper is organized as follows: the simulation procedure is outlined in Sec. II and the results briefly described in Sec. III. Section IV formalizes the implied mechanism for electron relaxation and the solutions to the corresponding differential equations. The results obtained in application to the simulated data are discussed in Sec. V. The conclusions of this work, and future directions are summarized in the last section.

II. SIMULATION PROCEDURE

Details of the simulation procedure have been described in previous publications,[11–14] thus we give here only a brief summary. There are four essential features of the simulation. (1) The water bath consists of 200 flexible SPC water molecules[15] in a cubic cell, at a density of 0.997 g/cm^3 at 300 K. Intramolecular potentials of the water molecules allow classical O–H bond stretches and changes in the equilibrium H–H distance. The constants are chosen to reproduce fundamental vibrational frequencies and the O–H dissociation energy in liquid water. The configuration of the water bath evolves with classical dynamics. (2) The electron is represented by its time-dependent Schrödinger equation in the solvent field. (3) The interaction between water molecules and the electron combines electrostatic and polarization potentials within a suitable pseudopotential. (4) The nonadiabatic algorithm consists of a stochastic surface hopping between adiabatic eigenstates,[18] as well as an appropriate semiclassical force on the solvent.[19]

Initial states of the water bath have been taken from a long (~200 ps) molecular dynamics run of pure water equilibrated at 300 K, at widely separated time intervals. The initial state of the electron has been taken to be a (delocalized) energy eigenstate of the zero time solvent configuration. The temporal evolution of this system was then followed by 1 fs time step, up to 400 fs. (The electron has been localized and relaxed to the ground state within this time, except for one single run out of 40.) Twenty trajectories have been run with the injected electron having approximately 2 eV excess energy, and 20 others where the initial excess energy of the electron was higher by about 0.5 eV.

III. SIMULATION RESULTS

The primary results of the simulations are the set of 40 solvent and electronic state trajectories in phase space of the above described system. Each trajectory contains the sequence of states, recorded at one femtosecond time intervals. While the basic behavior has been presented and discussed elsewhere,[14] there is a great deal more information in these trajectories. Here we focus our attention on some specific features of the trajectories that reveal the kinetic mechanism of the reaction in the computer experiments, and on the series of data extracted from the trajectories that can be used to estimate the kinetic parameters involved in this mechanism.

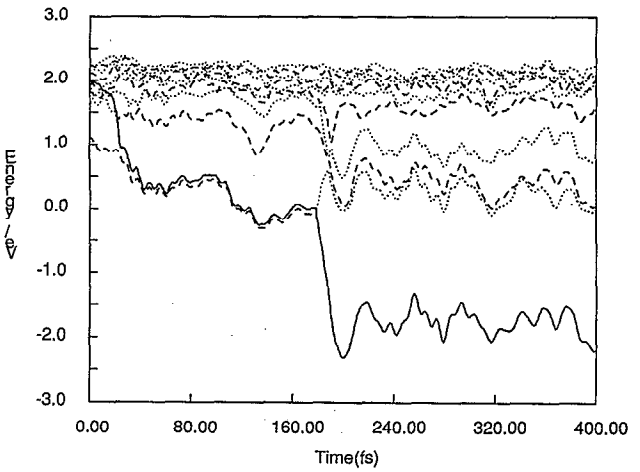

FIG. 1. Nonadiabatic trajectory (solid curve) along with the history of other (unoccupied) eigenstates (dashed curves) of an electron having an initial excess energy of ~2 eV. This curve is typical of electron trapping in a *p*-like excited state and then relaxing to the ground state. (Two-step process.)

A set of trajectories which manifest the principal behaviors are shown in Figs. 1–4. In each figure, the energies of the instantaneous adiabatic eigenstates of the electron are shown as a function of time. At zero time, the energies of the electron's eigenstates can be seen in the *unperturbed* solvent. From this time on, both the solvent and the electron evolve, mutually responding. After each time-step, the instantaneous adiabatic eigenstate energies are shown, according to the actual solvent configuration. In addition, the eigenstate marked with a *solid curve* denotes the one that is occupied by the electron. Due to the solvent fluctuations, there is necessarily a fluctuation of all the energy levels as time evolves.

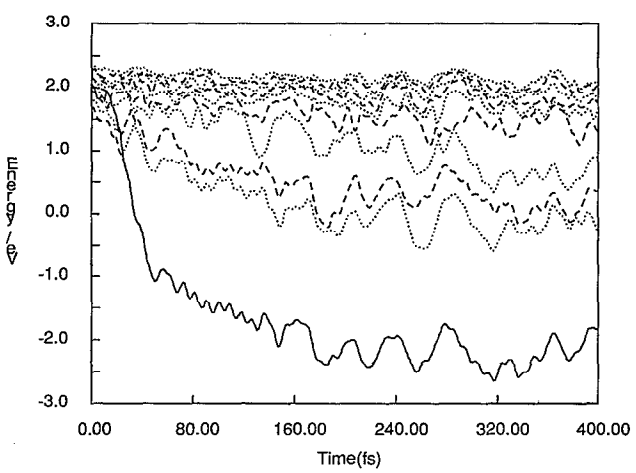

FIG. 2. Same diagram as in Fig. 1, showing a typical example of direct trapping, with an initial energy of ~2 eV.

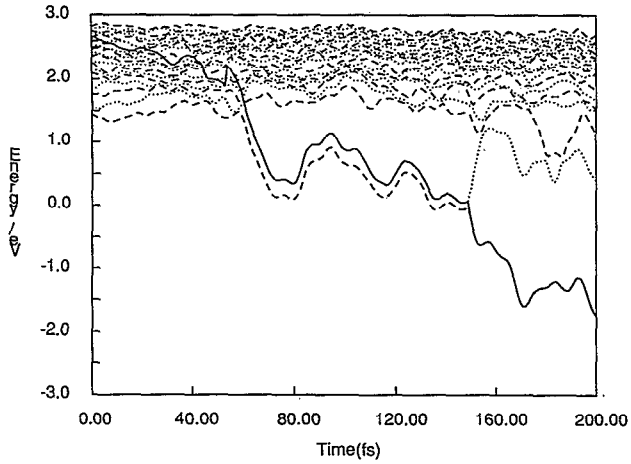

FIG. 3. Same diagram as in Fig. 1, a typical example of a two-step process for an electron with an initial excess energy of ~2.5 eV.

The most striking difference between individual trajectories is that, in some of them, there is a relatively fast relaxation to the lowest lying (*s*-like)[13] *localized ground state* (Figs. 2 and 4), while others (Figs. 1 and 3) show a fast relaxation to a (*p*-like)[13] *localized excited state* first, and then a final relaxation to the localized ground state. However, there are also similarities between the trajectories. In both cases it takes some 20 fs for the solvent to (energetically) relax around the freshly trapped electron. Also in both cases, there is an initial loss of energy in a cascade of mostly downwards transitions from one eigenstate to another. This behavior is characteristic of the trajectories where the initial excess energy of the electron is about 2 eV, as well as for those with some 2.5 eV initial excess energy, but there are quantitative differences between these two cases. Space and Coker have found rather similar localization trajectories in a recent simulation in liquid helium.[20] As we can already see from the figures, the initial energy loss through the manifold of the delocalized

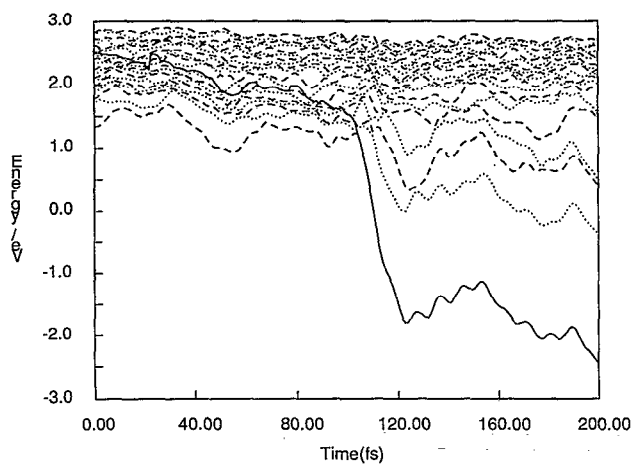

FIG. 4. Same diagram as in Fig. 1, showing a typical direct hydration process for an electron with an initial excess energy of ~2.5 eV.

TABLE I. Comparison of time intervals needed for different dynamic events during the localization of electrons in the simulation. Characteristic times shown are mean values calculated from 20 runs for both initial conditions. Numbers in brackets after the mean indicate the number of cases the event occurred (out of 20 runs). Numbers with ± sign in parentheses indicate the 95% confidence interval of the mean, calculated from the sample standard deviation and Student's *t* values.

Characteristic time, fs	~2 eV initial excess energy	~2.5 eV initial excess energy
Thermalization + trapping in the excited state	30.5[8] (±13.4)	58[4] (±27)
Excited state lifetime	164[8] (±130)	113[4] (±130)
Thermalization + trapping in the ground state	25.75[12] (±5.5)	77[16] (±22)

excited states takes longer for higher energy electrons. Although localization times and the lifetime of the localized excited species vary quite a lot among individual trajectories, they are also significantly different for trajectories of lower compared to higher initial energy electrons. (See Table I.)

These results, taken together, suggest a kinetic mechanism for the hydration of the electron in the simulations, which is discussed in the following section.

IV. MECHANISM OF ELECTRON HYDRATION

Before setting down the hydration mechanism, let us define some simple terms for the sake of brevity. We shall call the fully relaxed ground state electron as the *hydrated electron* and denote it by e^-_{aq}. The *excited localized electron* will be denoted by e^-_*. Electrons in one of the states of the delocalized manifold will be classified in two categories. *Hot electrons* are those which are unable to be localized in a suitable trap without losing some of their energy within the manifold, denoted by e^-_{hot}. *Free electrons* are those delocalized electrons which can directly be trapped without entering other states of the manifold, denoted by e^-_{free}. Using this notation, on the basis of the simulation results, we can write the scheme of the hydration mechanism as

$$e^-_{hot} \rightarrow \rightarrow \rightarrow \rightarrow e^-_{free} \xrightarrow{\text{trapping}} e^-_* \xrightarrow{\text{relaxation}} e^-_{aq}$$
$$\text{trapping} + \text{relaxation}. \qquad (1)$$

Let us further refine this mechanistic scheme introducing some additional conditions to facilitate a quantitative description. Suppose that the "thermalization" takes place as a downcascade energy loss proceeding from the ith to the $(i-l)$th excited state in the manifold. Suppose that any of these energy losses as well as the trapping, the relaxation, and the direct trapping *plus* relaxation can be considered as exponential decay phenomena (first order kinetics). Rewriting scheme (1) in this form, we get

$$e_1^- \xrightarrow{T_{th}} \cdots \xrightarrow{T_{th}} e_n^- \xrightarrow{T_{th}} e_{free}^- \xrightarrow{T_1} e_*^- \xrightarrow{T_2} e_{aq}^-, \quad e_{free}^- \xrightarrow{T_3} e_{aq}^- \tag{2}$$

In scheme (2) we treat the thermalization as an n-step process, with each step having the same characteristic time T_{th}, where $k_{th}=1/T_{th}$ is the probability per unit time of energy loss. We keep T_1 and T_2 to have the same meaning (i.e., the *localization time* and the *lifetime* of species e_*^-) as for the subprocess $e_{free}^- \rightarrow e_*^- \rightarrow e_{aq}^-$ invoked in the publications on experimental results.[3–8]

The system of differential equations corresponding to mechanism (2) is solved in the Appendix. The resulting concentration functions are

$$c_1=c_0 \cdot e^{-k_{th}t} \tag{3}$$

$$\vdots$$

$$c_i=\frac{c_0}{(i-1)!} \cdot (k_{th}t)^{i-1} \cdot e^{-k_{th}t}, \quad 1<i\leqslant n \tag{4}$$

$$\vdots$$

$$c_{free}=c_0\left(\frac{k_{th}}{k_{th}-k_1-k_3}\right)^n \times\left\{e^{-(k_1+k_3)t}-e^{-k_{th}t}\sum_{i=0}^{n-1}\frac{[(k_{th}-k_1-k_3)t]^i}{i!}\right\}, \tag{5}$$

$$c_*=c_0k_1\left(\frac{k_{th}}{k_{th}-k_1-k_3}\right)^n\left\{\frac{1}{k_2-k_1-k_3}\times[e^{-(k_1+k_3)t}-e^{-k_2t}]-\sum_{i=0}^{n-1}\frac{(k_{th}-k_1-k_3)^i}{(k_{th}-k_2)^{i+1}}\times\left[e^{-k_2t}-e^{-k_{th}t}\sum_{m=0}^{i}\frac{([k_{th}-k_2]t)^m}{m!}\right]\right\}, \tag{6}$$

$$c_{aq}=c_0\left[1-e^{-k_{th}t}\sum_{j=0}^{n-1}\frac{(k_{th}t)^j}{j!}\right]-c_{free}-c_*. \tag{7}$$

In expressions (3) to (7), c_0 is the concentration of the excess electrons injected at $t=0$ (i.e., the concentration of the species e_1^-), and a subscripted k is the inverse of the equivalent T.

V. RESULTS AND DISCUSSION

To test the validity of the mechanism proposed in the previous section for the simulation results, we can try to fit the concentration functions to the "experimental" *population curves* found by simulation. To find a particular population curve, those states which can be classified as the corresponding electronic species must be culled out of the 20 runs at each time step. While it is evident what should be counted as e_{aq}^- or e_*^-, there is an ambiguity in deciding whether a certain state in the manifold is still e_{hot}^-, or already e_{free}^-. To overcome this ambiguity, we counted both e_{hot}^- and e_{free}^- (i.e., neither e_{aq}^- nor e_*^-) together, and considered them as $e_{hot}^- + e_{free}^-$ when constructing the population curves. Population curves obtained with this method of culling (Figs. 5 and 6) are the data that can be used to compare the suggested mechanism to the results of the computer experiment, and, in case of a satisfying match, they can be used to estimate the kinetic parameters T_{th}, T_1, T_2, and T_3 in mechanism (2).

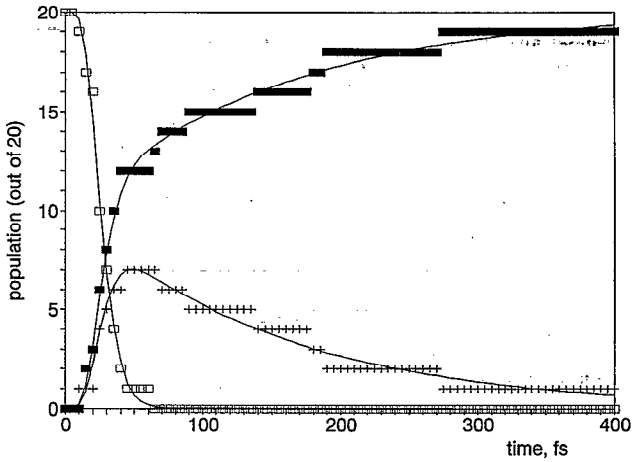

FIG. 5. Evolution of electron populations in 20 trajectories where the electron has an initial excess energy of ~2 eV. Symbols show the counts from the simulation: □ is the sum of e_{hot}^- and e_{free}^- electrons, + is the number of e_*^- electrons, and ■ is the number of e_{aq}^- species. Solid curves show the calculated values using mechanism (2) and estimated parameters of Table II.

To fit the mechanism, we used population curves sampled at 5 fs intervals. The matching of the fitted curves to the sampled data can be seen in Figs. 5 and 6. We can see an excellent fit for the case of the lower initial excess energy electrons (Fig. 5), and a good fit for the higher initial excess energy electrons (Fig. 6). A statistical goodness of fit test shows greater than 99% confidence for the acceptance of a match in both cases. Consequently, we can accept mechanism (2) to be valid, and use the simulation

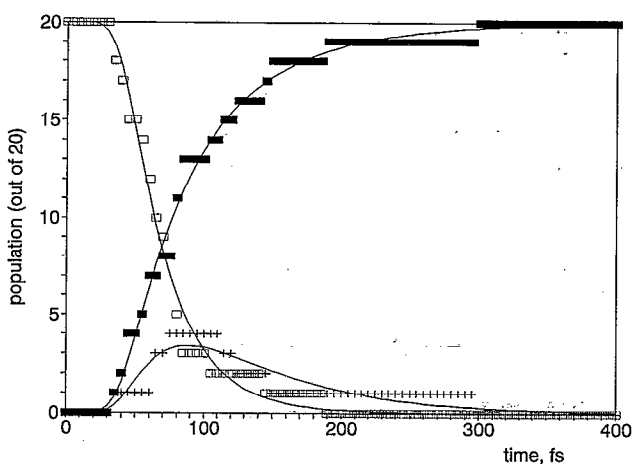

FIG. 6. Evolution of electron populations with the electron having an initial excess energy of ~2.4 eV. For the explanation of symbols, see Fig. 5.

TABLE II. Comparison of the kinetic parameters of mechanism (2) for both initial conditions, estimated from population curve data (Figs. 5 and 6), in femtosecond units. Numbers with ± sign in parentheses indicate the estimated 95% confidence intervals based on the Hessian matrix and the residual error in the nonlinear least squares procedure. Note that the branching ratio T_1/T_3 gives the direct hydration/two-step hydration ratio, as the probability per unit time of a reaction is $k=1/T$.

Parameter	~2 eV initial excess energy	~2.5 eV initial excess energy
T_1 (fs)	16 (±5)	92 (±10)
T_2 (fs)	148 (±6)	67 (±7)
T_3 (fs)	12 (±4)	48 (±4)
T_{th} (fs)	3.5 (±0.4)	3.1 (±0.13)
T_1/T_3 (Branching ratio)	55:45	65:35
Overall thermalization time (fs)	20 (±2.5)	40 (±1.6)

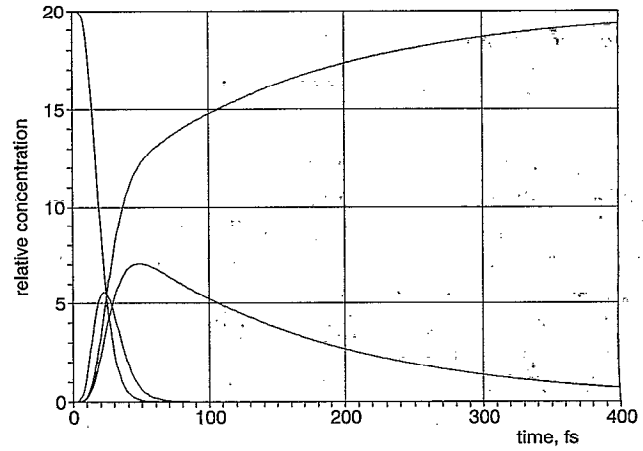

FIG. 7. Calculated time dependent concentration functions of the four electronic species e^-_{hot}, e^-_{free}, e^-_*, and e^-_{aq} corresponding to mechanism (2) and the parameters shown in Table II, for electrons with an initial excess energy of ~2 eV. The concentration scale is normalized to 20 to facilitate comparison with Fig. 5.

results to estimate the kinetic parameters involved in scheme 2. The estimated parameters are summarized in Table II.

The nonlinear least squares algorithm of Marquardt,[21] which was used for the estimation, is essentially a method to estimate *continuous* parameters. As the number of energy loss steps n, involved in scheme (2), is strictly integer, we kept it constant in the model function used in the least squares procedure, and compared the results of runs according to different values of n. In each case, we tried the highest physically meaningful value, which was the quantum number of the excited eigenstate of the manifold, where the electron was injected. This was $n=6$ for the lower, and $n=15$ for the higher excess energy electron.[14] Then we decreased n and checked for the resulted statistics. For the lower initial energy case, no other values gave as good a fit as $n=6$, and the estimated error of T_{th} sharply increased even for $n=5$. For the higher initial energy electron, any value between $n=11$ and $n=15$ gave practically the same quality of fit, and the errors of T_{th} were such that the value of $n \cdot T_{th}$ and its computed error had about the same value. This means that the *overall thermalization time* can be estimated from the "experimental" data, while the mechanism is not very sensitive to the actual value of n, unless it is greater than 10. This might also mean that, with a longer thermalization time, the probability of trapping increases for continuum states higher than $n=0$ or $n=1$. Results in Table II were obtained with $n=13$, an intermediate between the extremes 11 and 15.

A few more words about the relation between T_{th} and the overall thermalization time are appropriate. In many usual treatments,[22] thermalization is described by some particular mechanism, and a distribution of thermalization times is associated with the actual procedure. In the case of scheme (2), we suppose a *Poissonian process* for the energy loss, and n such processes are coupled in a cascade. Obviously, for one single energy loss, the distribution of thermalization times is exponential, with the expectation T_{th}. As the n subprocesses are independent, the expectation of the overall thermalization time is $n \cdot T_{th}$, but this is no longer exponentially distributed. Moreover, this characteristic time $n \cdot T_{th}$ loses its original interpretation of being the time after which the population is decreased by a factor of $1/e$. Instead, this factor is $1.212/e$ for $n=6$ and $1.259/e$ for $n=13$. In the Appendix, we give the distribution of thermalization times for a cascade of n energy losses.

Although mechanism (2) contains the species e^-_{free}, it is not possible to determine the population unambiguously from the simulation results, as we have mentioned before. However, the parameters T_{th}, T_1, and T_3 contain all the information necessary to calculate the concentration of e^-_{free} as well. This is shown, along with the other three concentration curves, in Figs. 7 and 8. The four concentration curves reveal substantial differences between the two cases. With lower initial energy electrons, there is a short dwell time in the manifold of continuum states, a quickly estab-

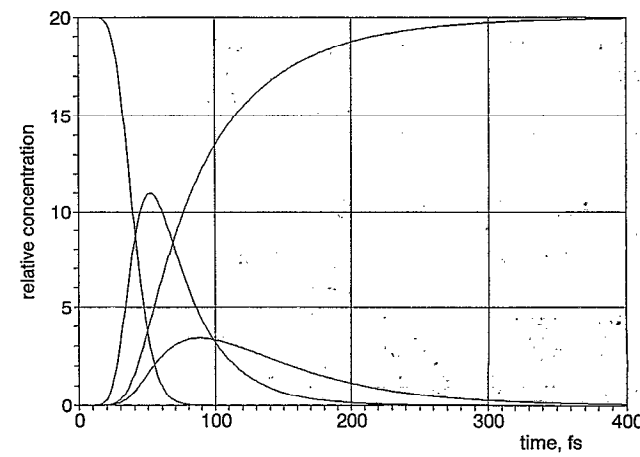

FIG. 8. Calculated time dependent concentration functions of the four electronic species e^-_{hot}, e^-_{free}, e^-_*, and e^-_{aq} corresponding to mechanism (2) and the parameters shown in Table II, for electrons with an initial excess energy of ~2.5 eV. The concentration scale is normalized to 20 to facilitate comparison with Fig. 6.

lished e^-_{free} population, and a high probability of the formation of both trapped states, e^-_* and e^-_{aq}. With higher initial energy electrons, there is a long dwell time in the continuum states, and a slower build-up of the reactive e^-_{free} population, but a much lower probability of the formation of either trapped states. Contrary to the previous case, where the "stocked" intermediate species is the trapped e^-_*, here the stocked e^-_{free} population largely exceeds that of the e^-_* up to 100 fs. In spite of these differences, branching ratios seem not to change much from one case to the other. It should be noted that the estimation of the ratio T_1/T_3 is rather uncertain; the two ratios 55:45 and 65:35 do not show a significant difference.

VI. CONCLUSIONS

In this article we have used the results of nonadiabatic quantum dynamics simulations of the relaxation of excited state electrons in water to develop a physically motivated kinetic model for this relaxation process. The corresponding differential equations were solved and it was shown that the kinetic model was able to produce a good description of the state populations seen in the computer experiment. The model extends beyond those used in published treatments of experimental data[3–8] in explicitly including both an initial thermalization step and an alternative, direct, pathway from the continuum to the ground state, both of which make important contributions in the simulated kinetics.

It is now of interest to consider the application of this more complete kinetic model to analysis of the alternative experimental data sets available.[3–8] This analysis, along with a full development of the spectral results that would be observed from the simulated data will be presented separately.

ACKNOWLEDGMENTS

E. Keszei is a beneficient of a grant by the National Research Fund of Hungary under Contract No. OTKA 4187, which is gratefully acknowledged. P. J. Rossky gratefully acknowledges grant support from the Robert A. Welch Foundation (F-0761) and from the Office of Naval Research, as well as the generous computational support of the Center for High Performance Computing of The University of Texas System.

APPENDIX: SOLUTION OF THE DIFFERENTIAL EQUATION ASSOCIATED WITH MECHANISM (2)

For the sake of clarity we use a slightly different notation here compared to the main text. The suggested reaction scheme can be rewritten as follows:

$$A_1 \xrightarrow{\alpha} \cdots \xrightarrow{\alpha} A_n \xrightarrow{\alpha} B \xrightarrow{\beta} C \xrightarrow{\gamma} D, \quad B \xrightarrow{\beta'} D \tag{A1}$$

The corresponding concentrations will be denoted by the respective lower-case letters $a_1, a_2, a_3 \cdots a_n$, b, c, and d.

The initial conditions to be considered are

$$a_1|_{t=0}=a_0,$$
$$a_2|_{t=0}=a_3|_{t=0}=\cdots a_n|_{t=0}=b|_{t=0}=c|_{t=0}=d|_{t=0}=0. \tag{A2}$$

The system of differential equations related to scheme (A1) can now be written in the form

$$\frac{da_1}{dt}+\alpha a_1=0, \tag{A3}$$

$$\frac{da_2}{dt}+\alpha a_2=\alpha a_1(t), \tag{A4}$$

$$\frac{da_3}{dt}+\alpha a_3=\alpha a_2(t) \tag{A5}$$

$$\vdots$$

$$\frac{da_n}{dt}+\alpha a_n=\alpha a_{n-1}(t), \tag{A6}$$

$$\frac{db}{dt}+(\beta+\beta')b=\alpha a_n(t), \tag{A7}$$

$$\frac{dc}{dt}+\gamma c=\beta b(t), \tag{A8}$$

$$\frac{dd}{dt}=\beta' b(t)+\gamma c(t). \tag{A9}$$

The above system of equations can be solved in a consecutive way starting with Eq. (A3), the solution of which is obviously

$$a_1=a_0e^{-\alpha t} \tag{A10}$$

and then substituting this solution into the right-hand side of the next equation and so on.

Keeping this in mind, Eqs. (A4)–(A8) will assume the following form:

$$\frac{dy}{dt}+\lambda y=\varphi f(t), \tag{A11}$$

where λ and φ are constant and $f(t)$ is a known function of time.

Note that Eq. (A11) is a special case of the inhomogeneous equation

$$\frac{dy}{dt}+p(t)y=q(t)$$

the solution of which is[23]

$$y=\exp\left[-\int_0^t p(x)dx\right]\int_0^t q(x)\exp\left[\int_0^x p(z)dz\right]dx.$$

Applying the above formula to Eq. (A11) we get:

$$y=\varphi e^{-\lambda t}\int_0^t f(x)e^{\lambda x}\,dx. \tag{A12}$$

The actual calculation of a_2 and a_3 from Eqs. (A4), (A5), and (A10) on the basis of Eqs. (A11) and (A12) leads to the intuitive conclusion that the general form of a_j must be

$$a_j=a_0\frac{(\alpha t)^{j-1}}{(j-1)!}e^{-\alpha t}\quad(j=1,2,3,\cdots n) \tag{A13}$$

as can be proved by induction.

Applying Eqs. (A13), (A11), and (A12) to Eq. (A7) we get

$$b=a_0\frac{\alpha^n}{(n-1)!}e^{-(\beta+\beta')t}\int_0^t x^{n-1}e^{-(\alpha-\beta-\beta')x}\,dx. \tag{A14}$$

Consecutive steps of integration by parts lead to the conclusion that

$$\int_0^t x^m e^{-\lambda x}\,dx=\frac{m!}{\lambda^{m+1}}\left[1-e^{-\lambda t}\sum_{l=0}^{m}\frac{(\lambda t)^l}{l!}\right]. \tag{A15}$$

One can use induction to prove the correctness of the above formula.

Applying Eq. (A15) to Eq. (A14) we get after some pencil pushing

$$b=a_0\left(\frac{\alpha}{\alpha-\beta-\beta'}\right)^n\left\{e^{-(\beta+\beta')t}-e^{-\alpha t}\sum_{i=0}^{n-1}\frac{[(\alpha-\beta-\beta')t]^i}{i!}\right\}. \tag{A16}$$

Let us apply now Eqs. (A16), (A11), and (A12) to Eq. (A8). We get

$$c=a_0\beta\left(\frac{\alpha}{\alpha-\beta-\beta'}\right)^n e^{-\lambda t}\left\{\frac{e^{-(\gamma-\beta+\beta')t}-1}{\gamma-\beta-\beta'}-\sum_{i=0}^{n-1}\left[\frac{(\alpha-\beta-\beta')^i}{i!}\int_0^t x^i e^{-(\alpha-\gamma)x}\,dx\right]\right\}.$$

Using again Eq. (A15) we can eliminate the integral from the above expression

$$c=a_0\beta\left(\frac{\alpha}{\alpha-\beta-\beta'}\right)^n\left\{\frac{e^{-(\beta+\beta')t}-e^{-\gamma t}}{\gamma-\beta-\beta'}-\sum_{i=0}^{n-1}\left[\frac{(\alpha-\beta-\beta')^i}{(\alpha-\gamma)^{i+1}}\left(e^{-\gamma t}-e^{-\alpha t}\sum_{j=0}^{i}\frac{[(\alpha-\gamma)t]^j}{j!}\right)\right]\right\}. \tag{A17}$$

The concentration of D can be calculated without actually solving Eq. (A9). Instead of this we can use the condition:

$$d=a_0-\sum_{j=1}^{n}a_j-b-c.$$

Using Eq. (A13) and switching to a new summation index $i=j-1$, we get from the above condition:

$$d=a_0\left[1-e^{-\alpha t}\sum_{i=0}^{n-1}\frac{(\alpha t)^i}{i!}\right]-b-c. \tag{A18}$$

One might also be interested in knowing just how long it takes for the average particle to get through the thermalization stages described by Eqs. (A3)–(A6) so that it can enter the chain of reactions described by Eqs. (A7)–(A9). Note that in Eq. (A18) the expression in brackets means the time-dependent fraction of particles which have passed through thermalization. At $t=0$ it starts from 0 and then it increases monotonically to 1 as t approaches infinity. In other words it can be considered as the (cumulative) distribution function of the related probability problem

$$F(t)=1-e^{-\alpha t}\sum_{i=0}^{n-1}\frac{(\alpha t)^i}{i!}. \tag{A19}$$

The corresponding density function is obtained by the differentiation of Eq. (A19)

$$\frac{dF}{dt}=\alpha e^{-\alpha t}\frac{(\alpha t)^{n-1}}{(n-1)!}. \tag{A20}$$

The expectation value of the time spent by the particle in the thermalization stages is

$$\tau=\int_0^\infty t\frac{dF}{dt}\,dt=\frac{\alpha^n}{(n-1)!}\int_0^\infty t^n e^{-\alpha t}\,dt. \tag{A21}$$

Using Eq. (A15) we can evaluate the integral in Eq. (A21)

$$\tau=\frac{\alpha^n}{(n-1)!}\frac{n!}{\alpha^{n+1}}\lim_{t\to\infty}\left[1-e^{-\alpha t}\sum_{i=0}^{n}\frac{(\alpha t)^i}{i!}\right].$$

Thus we get

$$\tau=\frac{n}{\alpha}. \tag{A22}$$

According to this result each thermalization stage increases the retention time by the same amount α^{-1}, the characteristic time of reaction (A3), i.e., the time the unreacted fraction of a_0 takes to drop to e^{-1}. Note, however, that since Eq. (A20) is not purely exponential, for $n>1$ we have lost this simple interpretation of τ. We can easily derive from Eq. (A20), that the fraction of particles still dwelling in the thermalization stages at time τ is

$$r=\frac{1}{e}\left(\sum_{i=0}^{n-1}\frac{n^i}{i!}\right)\Big/e^{n-1}.$$

For example, for $n=6$, this fraction increases to $1.212/e$.

[1] J. M. Wiesenfeld and E. P. Ippen, Chem. Phys. Lett. **73**, 47 (1980).
[2] D. N. Nikogosyan, A. A. Oraevsky, and V. I. Rupasov, Chem. Phys. **77**, 131 (1983).
[3] Y. Gauduel, A. Migus, J. L. Martin, Y. Lecarpentier, and A. Antonetti, Ber. Bunsenges. Phys. Chem. **89**, 218 (1985); A. Migus, Y. Gauduel, J. L. Martin, and A. Antonetti, Phys. Rev. Lett. **58**, 1559 (1987).
[4] Y. Gauduel, S. Pommeret, A. Migus, and A. Antonetti, Radiat. Phys. Chem. **34**, 5 (1989); J. Phys. Chem. **93**, 3880 (1989).
[5] Y. Gauduel, S. Pommeret, A. Migus, N. Yamada, and A. Antonetti, J. Am. Chem. Soc. **112**, 2925 (1990).
[6] F. H. Long, H. Lu, and K. B. Eisenthal, J. Chem Phys. **91**, 4413 (1989).
[7] F. H. Long, H. Lu, and K. B. Eisenthal. Phys. Rev. Lett. **64**, 1469 (1990).
[8] F. H. Long, H. Lu, and K. B. Eisenthal. J. Opt. Soc. Am. B **7**, 1511 (1990).
[9] J. Schnitker, P. J. Rossky, and G. A. Kenney-Wallace, J. Chem. Phys. **85**, 2986 (1986).
[10] P. J. Rossky and J. Schnitker, J. Phys. Chem. **92**, 4277 (1988).
[11] J. C. Tully, J. Chem. Phys. **93**, 1061 (1990).

[12] F. A. Webster, P. J. Rossky, and R. A. Friesner, Comput. Phys. Commun. **93**, 494 (1991).
[13] F. A. Webster, J. Schnitker, M. S. Friedrichs, R. A. Friesner, and P. J. Rossky, Phys. Rev. Lett. **66**, 3172 (1991).
[14] T. H. Murphrey and P. J. Rossky, J. Chem. Phys. **99**, 515 (1993).
[15] K. Toukan and A. Rahman, Phys. Rev. B **31**, 2643 (1985).
[16] C. Romero and C. D. Jonah, J. Chem Phys. **90**, 1877 (1989).
[17] R. B. Barnett and U. Landmann, J. Chem. Phys. **90**, 4413 (1989).
[18] J. C. Tully and R. K. Preston, J. Chem. Phys. **55**, 562 (1971).
[19] P. Pechukas, Phys. Rev. **181**, 174 (1969).
[20] B. Space and D. F. Coker, J. Chem. Phys. **96**, 652 (1992).
[21] D. W. Marquardt, J. Soc. Ind. Appl. Math. **11**, 431 (1963).
[22] R. Schiller, in *Excess Electrons in Dielectric Media*, edited by C. Ferradini and J.-P. Jay-Gerin (CRC, Boca Raton, 1991), p. 105 and references cited therein.
[23] J. B. Fraleigh, *Calculus* (Addison-Wesley, New York, 1990), p. 931.